International Journal of Modern Physics B, Vol. 15, Nos. 19 & 20 (2001) 2707–2717

STATICS AND DYNAMICS OF COUPLED ELECTRON–PHONON SYSTEMS

S. A. TRUGMAN*,†, J. BONČA† and LI-CHUNG KU*

*Theory Division, Los Alamos National Laboratory, Los Alamos, NM 87545, USA
†FMF, University of Ljubljana and J. Stefan Institute, 1000, Slovenia

We review recent variational methods that provide extremely accurate solutions for the problem of one and two electrons coupled to dynamical, quantum phonons, including retardation effects. The dynamics of these systems far from equilibrium is explored, including the dynamics of polaron formation after electron injection by an STM. An examination of three-point functions suggests a qualitative modification of the traditional picture of a polaron. Long-range electron–phonon interactions are studied in some generality, including vector and frustrated Fröhlich models, and bounds are obtained on the possible mass enhancement.

1. Introduction and Review

Many-body or correlated electron problems are difficult because the size of the Hilbert space grows exponentially with both the number of particles and the spatial extent of the system. The static ground state properties remain unknown even for some of the simplest and most studied correlated electron systems. It is not known, for example, whether the repulsive Hubbard model superconductors in various angular momentum channels, whether it forms stripes, or whether it is a fermi liquid. The dynamics of these models are even further out of reach. There are, however, certain many-body systems for which ground-state correlations can be calculated to very high accuracy. Information about excited states and dynamics far from equilibrium can also be obtained. Perhaps surprisingly, this information can be obtained for spatially infinite systems, in spite of the fact that this limit generally causes an exponential increase in difficulty.

The systems that can be treated in this way generally involve the motion of one or two or a few particles or "defects" in a background that is well-understood in the absence of defects. Examples that have been studied include the dynamics and interactions of holes in an antiferromagnetic insulator,[1] with applications to doped Mott insulators such as high temperature superconductors. The holes are surrounded by a cloud of spin-flips as they move and become nontrivial quasiparticles. They can also form bound states. Other examples are the Holstein or Fröhlich or SSH polarons and bipolarons, in which one or two electrons interact with phonons. These are many-body problems in the sense that the electron becomes surrounded

by a large number of correlated phonon excitations as it moves. Two polarons may or may not form a bipolaron bound state, depending on the strength of the electron–phonon coupling, the electron hopping amplitude, and the Coulomb repulsion between them. We will focus here on the coupled electron–phonon problem. Applications of electron–phonon coupling, polarons, and bipolarons to high temperature superconductors and other materials are contained in Refs. 2 and 3.

The coupled electron–phonon system can be studied in a variational Hilbert space of phonon excitations in the vicinity of the electron on a spatially *infinite* lattice. The size of the variational Hilbert space can be increased to arbitrary size in systematic steps. As in most correlated electron problems, the size of the Hilbert space increases exponentially with the number of steps, which is the usual recipe for disaster. Unlike the usual case, however, the accuracy of the solution also increases exponentially with the number of steps. For intermediate coupling, the ground state energy is found to become approximately a factor of ten more accurate when the size of the Hilbert space doubles. This is a comparatively favorable return on computational effort. Intermediate coupling is in fact the most demanding regime, where approximations such as weak coupling perturbation theory, strong coupling perturbation theory, and the adiabatic and anti-adiabatic approximations fail, and where simple variational approaches often yield spurious first order phase transitions.

All eigenstates on the spatially infinite lattice can be chosen to have a good momentum $\mathbf{k}$, where the momentum can continuously assume any value (as opposed to discrete values on a finite lattice). In accordance with rigorous theorems,[4] we find that there is no phase transition in which the polaron ground state becomes "self trapped". The polaron mass can, however, increase rather rapidly (and smoothly) with electron–phonon coupling. In contrast, there is a true "phase transition" in the Raman active first excited state; its energy is nonanalytic in the electron–phonon coupling as a polaron and an additional phonon form a bound state.[5]

The properties of polarons, generally on finite lattices, have been calculated by a number of other methods, including perturbation theory,[6] variational methods,[7,8] exact diagonalization,[9,10] density matrix renormalization group,[11] Monte Carlo,[12] and others. These methods are generally less accurate and consume greater computational resources than the method described below. Some of these methods give variational energies (energies guaranteed greater than or equal to the true ground state energy) for the polaron on a finite lattice. The energies are not, however, variational on the infinite lattice, since the polaron energy is an increasing function of lattice size for periodic boundary conditions.

The Holstein Hamiltonian is

$$H = -t\sum_{js}(c^{\dagger}_{j+1,s}c_{j,s} + \text{H.c.}) - \lambda\sum_{js} c^{\dagger}_{j,s}c_{j,s}(a_j + a^{\dagger}_j) + \omega\sum_{j} a^{\dagger}_j a_j\,, \qquad (1)$$

where t is the electron hopping amplitude, λ is the electron–phonon coupling, and ω is the phonon frequency; all three have units of energy.

The variational Hilbert space is defined starting with a root state (the electron on site j with no phonon excitations), and operating repeatedly with the

off-diagonal terms λ and t of the Hamiltonian. The Hilbert space can be organized into generations, where generation M includes those states that require M operations of the off-diagonal matrix elements to be reached from the root state. The (unnormalized) basis states in the variational Hilbert space are given below, where $c_j^\dagger$ creates an electron on site j, and $a_j^\dagger$ creates a phonon on site j:

Generation 0: $c_j^\dagger|0\rangle$.
Generation 1: $a_j^\dagger c_j^\dagger|0\rangle$.
Generation 2: $a_j^\dagger a_j^\dagger c_j^\dagger|0\rangle,\ a_j^\dagger c_{j-1}^\dagger|0\rangle,\ a_j^\dagger c_{j+1}^\dagger|0\rangle$.
Generation 3: $a_j^\dagger a_j^\dagger a_j^\dagger c_j^\dagger|0\rangle,\ a_j^\dagger a_j^\dagger c_{j-1}^\dagger|0\rangle,\ a_j^\dagger a_j^\dagger c_{j+1}^\dagger|0\rangle,\ a_j^\dagger a_{j-1}^\dagger c_{j-1}^\dagger|0\rangle,\ a_j^\dagger c_{j-2}^\dagger|0\rangle,$
$a_j^\dagger a_{j+1}^\dagger c_{j+1}^\dagger|0\rangle,\ a_j^\dagger c_{j+2}^\dagger|0\rangle$.
...

Generation M includes states with up to M phonon excitations and phonons as far as $M-1$ sites from the electron. The Hilbert space includes all translations of the above states on an infinite lattice ($j = \ldots, -2, -1, 0, 1, 2, \ldots$), and all matrix elements between retained states, as shown in Fig. 1. The many-body problem is thus mapped onto a 1-body periodic tight-binding Hamiltonian with many basis states per unit cell. Using Bloch's theorem, the wavefunction can be taken to have a good momentum k, and is solved using an exact diagonalization or Lanczos method. Figure 1 illustrates a very small variational space of 7 states per unit cell; actual calculations are done with as many as 10^7 states per unit cell.

For large generation numbers, there are approximately twice as many states per unit cell (lattice site j) in generation $M+1$ as in generation M for spatial dimension 1. In d dimensions, there are $d+1$ times as many states in generation $M+1$ as in generation M. The bipolaron in 1D, which has two electrons plus phonons, has the same factor (two) as the polaron. The number of generations retained in

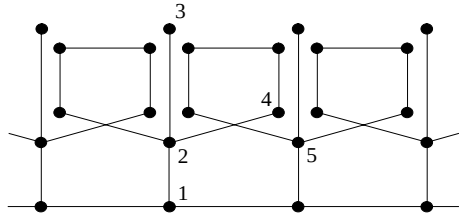

Fig. 1. The small variational Hilbert space shown for the polaron is a subset of the generation 3 space. Basis states in the many-body Hilbert space are represented by dots, and nonzero off-diagonal matrix elements by lines. The x-coordinate of the dots is (aside from small displacements) the coordinate of the electron. Vertical bonds create phonons, and horizontal or nearly horizontal bonds are electron hops. State $|1\rangle$ is an electron on site 0 and no phonons. State $|2\rangle$ is an electron and phonon, both on site 0. State $|4\rangle$ is an electron on site 1 and a phonon on site 0, which is reached from state $|2\rangle$ by hopping the electron to the right. State $|5\rangle$ is a translation of state $|2\rangle$. The Hamiltonian is sparse in this basis, with at most 4 bonds attached to a dot. The dots can also be thought of as Wannier orbitals in a one-body periodic tight-binding model.

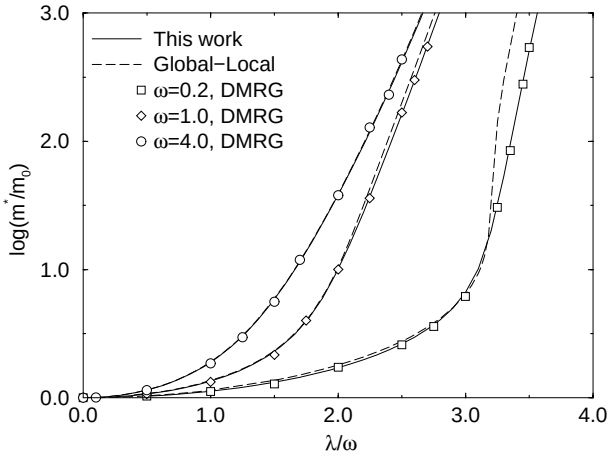

Fig. 2. The logarithm of the effective mass m^*/m_0 as a function of λ/ω. Our results are plotted as full lines, and Global-Local results as dashed lines.[8] Open symbols, indicating the value of ω, are DMRG results.[11]

a calculation is determined by computer resources and the desired accuracy. For example, the ground state ($k = 0$) polaron energy in 1D for $\lambda = \omega = t = 1$ is $E = -2.469684723933$, which is accurate to the number of digits shown and can be obtained in less than a minute on a small workstation. (One could obtain higher accuracy by working in extended precision.) The polaron mass can be calculated by numerically computing $\partial^2 E(k)/\partial k^2$, as shown in Fig. 2. Other correlation functions, as well as the "bands" that represent the ground and excited state many-body wavefunctions, are given in Ref. 5. Because this method is not as computationally demanding, it is straightforward to extend the calculations to dimensions 2 and 3.[13]

The properties of interacting polarons, including Coulomb repulsion and the exchange of quantum, dynamical, retarded phonons, can also be calculated. The bipolaron phase diagram, correlation functions, and isotope effect have been computed for the Hubbard–Holstein model,[14] and for longer range electron–phonon coupling.[15]

Nonlinear phonons: Strangely, the linear phonon spectrum of equally spaced energy levels (and linear electron–phonon coupling) are just arbitrary special cases for this variational method. A nonlinear phonon spectrum can be treated without additional effort. The special case of a deep double well, with two close tunnel-split low-lying levels, and the others high enough to be neglected, is computationally simpler than the linear phonon case. A limited amount of work has been done on this system, which remains light even at very large electron–phonon coupling.

2. Dynamics

Dynamical effects are implicitly included in the excited state eigenfunctions of the polaron problem.[5] Dynamics also plays a central role in inelastic tunneling

processes, in which an incoming electron encounters barriers and (possibly large) potential drops, while interacting with various phonons degrees of freedom. The electron can reflect or transmit in elastic and in many distinct inelastic channels, in which energy is deposited in phonon modes. These problems can all be solved essentially exactly if the number of scattering channels is not too large (less than the order of 10^7 channels for moderate computational resources).[16]

Another dynamical problem is the polaron driven by a strong electric field. In the absence of electron–phonon coupling, the electron localizes in Wannier–Stark ladders. In the presence of electron–phonon coupling, however, the electron can move downhill as it continually radiates phonons. A minimal Hilbert space for this problem is shown in Fig. 3. In contrast to the periodic Hilbert space shown in Fig. 1, this Hilbert space is self-similar, and constantly branching. The branches arise because the electron has choices about where to emit phonons. (Bonds x, y, and z are phonon emission processes, and a and b are electron hopping processes.) The (complex) scattering wavefunction can be obtained for this self-similar structure, which is not equivalent to standard Bethe lattices. As the electron's initial energy changes, it predominantly enters different branches. Various correlation functions, including the "damped" ringing of phonons in the wake of the electron, have been calculated.[17] The structure of the Hilbert space in Fig. 3 is a concrete realization of the notion that the "wave function of the universe" resides in a constantly branching space.[18a]

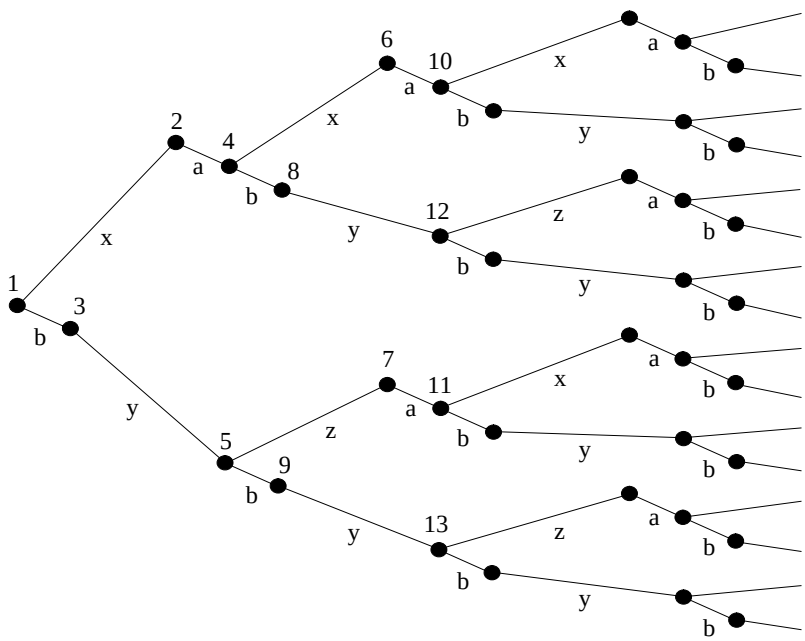

Fig. 3. A variational many-body Hilbert space similar to Fig. 1, except that a large electric field is included.

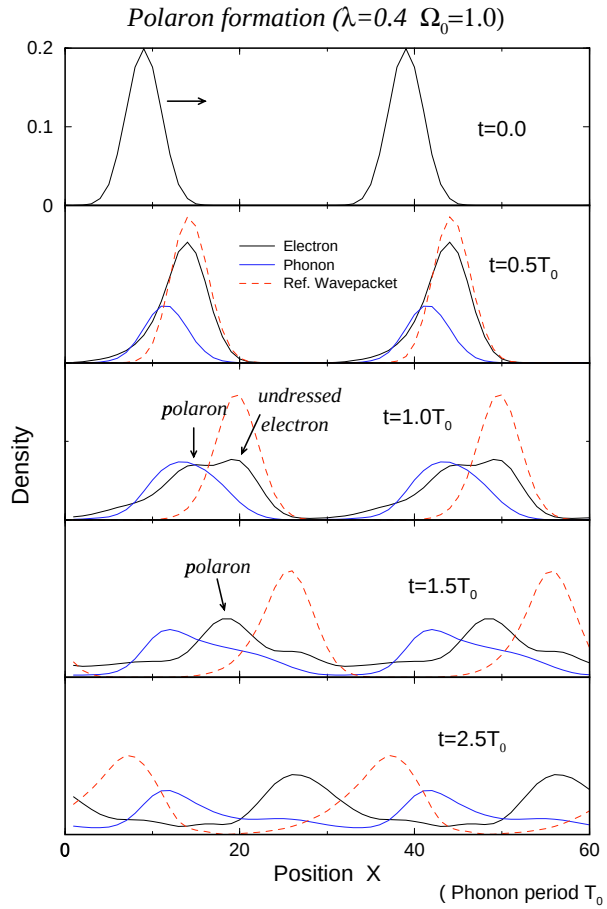

Fig. 4. A bare electron moving to the right is injected at time $t = 0$. The electron density $\langle c_j^\dagger c_j \rangle$ is plotted as a solid line, the phonon density $\langle a_j^\dagger a_j \rangle$ as a light solid line, and the reference wavepacket (the electron density if the electron–phonon coupling λ were set to zero) as a dashed line. The calculation is done on a 30-site periodic lattice, which is plotted twice to avoid having to mentally wrap the solution.

Another approach to solving dynamical problems, instead of computing scattering eigenfunctions, is to directly integrate the time-dependent Schrödinger equation

$$i\dot{\psi} = H\psi\,. \tag{2}$$

This has been implemented so far only on a finite lattice. An example is an electron injected into a material with electron–phonon coupling by a time-resolved STM tip.[18b] An initial bare electron wavepacket is launched to the right, as shown in the first frame taken from a movie, Fig. 4. (A wavepacket would also be launched to the left, but is not shown for clarity.) The electron wavepacket moves rapidly to the right. At time $t = 1.0T_0$, where T_0 is the phonon period, a second peak is visible in the electron density, which is the slower moving polaron quasiparticle peak. At

later times, the amplitude for the bare electron decreases, and that of the polaron increases.

3. Modified Toyozawa State

A simple variational wavefunction for the Holstein polaron was proposed by Toyozawa.[7] It is usually believed to be a correct qualitative and semi-quantitative description. One shortcoming is that the solution (and the polaron mass) changes discontinuously at certain parameters t, λ, and ω, where the correct solution is continuous. We will see that although the Toyozawa wavefunction gives a good account of the two-point functions, the three-point functions are wildly inaccurate.

The Toyozawa wavefunction is written as a product of phonon coherent states:

$$|\psi(k)\rangle = \sum_j e^{ikj} c_j^\dagger |0\rangle \cdots |z_{j-2}\rangle |z_{j-1}\rangle |z_j\rangle |z_{j+1}\rangle |z_{j+2}\rangle \cdots . \tag{3}$$

The state $|z_j\rangle$ is a coherent state[19a] of the phonon mode on site j. For real values of the number z, the phonon wavefunction is the harmonic oscillator groundstate displaced by an amount proportional to z. For momentum $k = 0$, the variational Toyozawa $z's$ are real and symmetric: $z_{j-m} = z_{j+m}$. The structure of the phonon cloud surrounding the electron can be investigated by calculating two-point, three-point (and higher) correlation functions,

$$\begin{aligned} \alpha_2(j) &= \langle\psi| c_m^\dagger c_m a_{m+j}^\dagger a_{m+j} |\psi\rangle \,, \\ \alpha_3(j,l) &= \langle\psi| c_m^\dagger c_m a_{m+j}^\dagger a_{m+j} a_{m+l}^\dagger a_{m+l} |\psi\rangle \,. \\ \cdots \quad \cdots & \qquad\qquad \cdots \end{aligned} \tag{4}$$

Because of the symmetry of the Toyozawa wavefunction, $\alpha_3(j,l) = \alpha_3(-j,l)$, $j \neq \pm l$. In the essentially exact numerical calculations in a large variational space, however, it is found that $\alpha_3(1,2)$ can exceed $\alpha_3(-1,2)$ by more than a factor of ten. This is a significant qualitative discrepancy. This result is made plausible by the fact that perturbing in t and λ, the first nonvanishing contribution to $\alpha_3(1,2)$ appears at order $\lambda^2 t^2$, whereas the first contribution to $\alpha_3(-1,2)$ is order $\lambda^2 t^4$; the electron must visit more sites in the latter case. This suggests that the picture of a polaron as a symmetric cloud of phonons surrounding an electron, Eq. (3), should be modified. It is more correct to write a polaron as a sum of two asymmetric clouds, one extending like a comet-tail primarily off to the right, and one extending to the left. This would capture the failure of $\alpha_3(j,l)$ to approximate $\alpha_3(-j,l)$. The suggested generalization of Eq. (3) has been quantitatively investigated.[19b]

4. Long–Range Electron–Phonon Coupling: Fröhlich Models

The Fröhlich model has long range electron–phonon coupling, whereas the Holstein model couples only to onsite phonons. Different local arrangements of ions are also possible. How are polaron (and bipolaron) properties affected by the details of the model?

A fairly general polaron Hamiltonian can be written

$$H = -t\sum_{js}(c^\dagger_{j+1,s}c_{j,s} + \text{H.c.}) - \omega g\sum_{jls} f_l(j)c^\dagger_{j,s}c_{j,s}(a_l + a^\dagger_l) + \omega\sum_l a^\dagger_l a_l\,, \quad (5)$$

where j sums over electron orbitals in a tight-binding lattice, l sums over phonon modes, $f_l(j)$ is proportional to the coupling of an electron on site j to phonon l, t is the electron hopping, and all phonons are assumed to have frequency ω. The Holstein model contains only local electron–phonon coupling, $f_l(j) = \delta_{l,j}$. In the Fröhlich Hamiltonian, long range electron–phonon coupling arises from the interaction of the electric field of the electron with the ionic coordinates.

We consider the analytic properties of various polaron models in the strong coupling limit, where the hopping t is considered a perturbation. When t is zero, the groundstate of the Hamiltonian Eq. (5) has the electron at an arbitrary site, and the phonon state on site l a coherent state[19] $|z_l\rangle = Ne^{z_l a^\dagger_l}|0\rangle$, where N is a normalization constant and z_l is in general a complex number, in this case real with $z_l = gf_l(j)$. To order t^0, the energy of the polaron is

$$E_p = -\omega\sum_l z_l^2\,. \quad (6)$$

The Z-factor is the dot-product squared of the polaron wavefunction with a bare electron wavefunction. It is the quasiparticle residue measured in photoemission, inverse photoemission, or tunneling, and is given by

$$Z = \exp\left(-\sum_l z_l^2\right)\,. \quad (7)$$

The leading effective mass correction appears at order t^1, and comes from the overlap of the phonon displacements before and after an electron hop,

$$m^* = \frac{m}{m_0} = \frac{t_0}{t} = \exp\left[\frac{1}{2}\sum_l (z_l - z_{l+1})^2\right]\,, \quad (8)$$

where t_0 is the bare hopping.

Regardless of the range and details of the interaction, the Z-factor is related to the polaron energy via

$$Z = e^{-E_\mathrm{p}/\omega}\,, \quad (9)$$

where E_p is taken as a positive number. (The long distance part of the sum converges in $d < 4$, since z_l is proportional to the electric field of a charge, which vanishes as r^{-2} at large r.) The effective mass m^*, in contrast, is not given simply in terms of the polaron energy (see also Ref. 9). It depends on the range of the interaction and on the details of the lattice arrangement at short distances. One can define a model-dependent parameter γ by $m^* = e^{\gamma E_\mathrm{p}/\omega}$. To leading order in t,

$$\gamma = \frac{1}{2}\sum_l (z_l - z_{l+1})^2 \Bigg/ \sum_l z_l^2\,. \quad (10)$$

The Holstein model, where each electron site couples to a single phonon site ($f_l(j) = \delta_{l,j}$), has $\gamma = 1$. Models with large γ generate heavy polarons that are likely to localize from disorder or mutual interactions, whereas a small γ leads to light polarons (and bipolarons) that are more likely to be itinerant or superconducting. Calculations beyond leading order in t require a Lang–Firsov similarity transformed Hamiltonian.[5,20]

Alexandrov and Kornilovitch[12] and Fehske *et al.*[9] have considered a Fröhlich model that is illustrated in Fig. 5(b), in which the ions can move only in the y-direction. In that case, $f_l(j) = b[b^2 + (j-l)^2]^{-3/2}$, where the line of ions is a distance b from the line of Wannier orbitals, and the Wannier orbitals are a distance 1 from each other. Evaluating the infinite sums in Eq. (10), one obtains $\gamma = 0.38732$ for $b = 1$, substantially reduced from the Holstein $\gamma = 1$. As the electron interacts with an increasingly number of neighboring sites $(1, 3, 5, 7, \ldots)$, γ decreases as $(1,\ 0.4343,\ 0.3915,\ 0.3880, \ldots)$, showing that the infinite distance result arises primarily from the nearest ions. Increasing the distance b from the electron to the ion sites results in smoother electron–phonon interactions and much lower γ (lighter mass). For example, $b = 2$ results in $\gamma = 0.10776$, and $b = 4$ gives $\gamma = 0.02864$, an extremely light polaron.

The lattice of Fig. 5(a) is identical to that of Fig. 5(b), except that the ions are shifted between the Wannier orbitals, as would be the case in certain oxides.[21] This shift reduces the $(b = 1)$ $\gamma = 0.38732$ for Fig. 5(b) to $\gamma = 0.28678$ for Fig. 5(a), which shows that the details of the short-distance ionic arrangement can have an effect on the polaron mass.

From Eq. (10), it is straightforward to obtain bounds for the maximum and minimum possible γ for an interaction extending over N sites:

$$1 - \cos(\pi/(N+1)) \le \gamma \le 1 - \cos(N\pi/(N+1))\,. \tag{11}$$

γ can thus become arbitrarily small, $O(N^{-2})$, but can never exceed 2. The lower bound for γ in Eq. (11) is achieved for an interaction $f_l(j) = \cos(\pi(l-j)/(N+1))$.

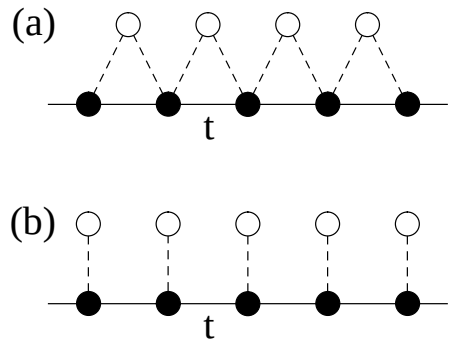

Fig. 5. Filled circles represent electron Wannier orbitals, open circles represent ions. In (a), ions are between and above the Wannier orbitals, whereas in (b), ions are directly above. Solid lines indicate overlap integral t between Wannier orbitals.

The upper bound is achieved for $f_l(j) = \cos(N\pi(l-j)/(N+1))$, which is the same function except that $f_l(j)$ alternates in sign. For example, an electron coupled to 5 phonon sites can have a γ ranging from 0.1340 to 1.866 .

In the Fröhlich model of Fig. 5(b), it was assumed that the ions can move only in the $\hat{y}$-direction. What would change in a more realistic vector model, where both $\hat{x}$ and $\hat{y}$ displacements are allowed? In this case, there are two independent phonon modes for each ion. The $\hat{x}$ displacements are *frustrated*, in the sense that ions displace in opposite directions on opposite sides of the electron, a fact that is even more relevant for Fig. 5(a). This increases the effective mass. The $\hat{x}$ interactions are also longer range than the $\hat{y}$ interactions, decaying as r^{-2} rather than r^{-3}, because the electric field is predominantly along the x-axis at large separations. The electron–phonon couplings are

$$\begin{aligned} f_l^x(j) &= (j-l)/[b^2+(j-l)^2]^{3/2}\,, \\ f_l^y(j) &= b/[b^2+(j-l)^2]^{3/2}\,. \end{aligned} \tag{12}$$

(If $f_l^x(j)$ were proportional to $f_l^y(j)$, γ would be unchanged compared to the latter alone.) A calculation to $O(t^1)$ reveals that for the lattice of Fig. 5(b), $b = 1$, γ increases from 0.38732 to only 0.40649 upon inclusion of the vector degree of freedom. This surprisingly modest increase reflects the facts that the y-displacements already comprise the largest part of the sums, and that neither the r^{-2} nor r^{-3} tails contribute significantly to the effective mass at large r.

Issues of electron–phonon as well as electron–spin coupling are relevant to ultrafast, time-resolved optical pump, teraherz probe experiments on CMR manganite thin films. These experiments demonstrate that phonon disorder dominates resistivity at low temperatures, while spin disorder dominates near T_c.[22]

Acknowledgment

We acknowledge stimulating discussions with A. N. Das, H. Fehske, V. V. Kabanov, and F. Marsiglio. This work was supported in by the US DOE and by the Slovene Ministry of Education, Science and Sport.

References

1. S. A. Trugman, *Phys. Rev.* **B37**, 1597 (1988); *Phys. Rev. Lett.* **65**, 500 (1990); *Phys. Rev.* **B41**, R892 (1990).
2. *Lattice Effects in High-T_c Superconductors*, eds. Y. Bar-Yam, T. Egami, J. Mustre de Leon and A. R. Bishop (World Scientific, Singapore, 1992).
3. E. K. H. Salje, A. S. Aleksandrov and W. Y. Liang, *Polarons and Bipolarons in High Temperature Superconductors and Related Materials* (Cambridge University Press, Cambridge, 1995). A. S. Alexandrov and N. F. Mott, *Rep. Progr. Phys.* **57**, 1197 (1994).
4. B. Gerlach and H. Lowen, *Rev. Mod. Phys.* **63**, 63 (1991).
5. J. Bonča, S. A. Trugman and I. Batistic, *Phys. Rev.* **B60**, 1633 (1999).
6. A. N. Das, this volume.

7. Y. Toyozawa, *Prog. Theor. Phys.* **26**, 29 (1961).
8. A. W. Romero, D. W. Brown and K. Lindenberg, *J. Chem. Phys.* **109**, 6540 (1998).
9. H. Fehske, J. Loos and G. Wellein, *Phys. Rev.* **B61**, 8016 (2000).
10. F. Marsiglio, *Physica* **C244**, 21 (1995).
11. E. Jeckelmann and S. R. White, *Phys. Rev.* **B57**, 6375 (1998).
12. A. S. Alexandrov and P. E. Kornilovitch, *Phys. Rev. Lett.* **82**, 807 (1999).
13. S. A. Trugman (unpublished).
14. J. Bonča, T. Katrašnik and S. A. Trugman, *Phys. Rev. Lett.* **84**, 3153 (2000).
15. J. Bonča and S. A. Trugman, cond-mat/0103457.
16. J. Bonča and S. A. Trugman, *Phys. Rev. Lett.* **75**, 2566 (1995).
17. J. Bonča and S. A. Trugman, *Phys. Rev. Lett.* **79**, 4874 (1997).
18. (a) W. H. Zurek, *Phys. Rev.* **D26**, 1862 (1982); (b) G. P. Donati, G. Rodriguez and A. J. Yaylor, *J. Opt. Soc. Am.* **B17**, 1077 (2000).
19. (a) L. S. Schulman, *Techniques and Applications of Path Integration*, Wiley (1981); (b) Li-Chung Ku *et al.*, unpulished.
20. I. G. Lang and Yu. A. Firsov, *Sov. Phys. JETP* **16**, 1301 (1963); *Sov. Phys. Sol. Stat.* **5**, 2049 (1964).
21. N. Tsuda, K. Nasu, A. Yanase and K. Siratori, *Electronic Conduction in Oxides* (Springer-Verlag, 1991).
22. R. D. Averitt, A. I. Lobad, V. Thorsmolle, A. J. Taylor, C. Kwon and S. A. Trugman, *Phys. Rev. Lett.* **87**, 017401 (2001).